

Solution of Inverse Boundary Optimization Problem by Trefftz Method and Exponentially Convergent Scalar Homotopy Algorithm

Hsin-Fang Chan¹, Chia-Ming Fan^{1,2} and Weichung Yeih¹

Abstract: The inverse boundary optimization problem, governed by the Helmholtz equation, is analyzed by the Trefftz method (TM) and the exponentially convergent scalar homotopy algorithm (ECSHA). In the inverse boundary optimization problem, the position for part of boundary with given boundary condition is unknown, and the position for the rest of boundary with additionally specified boundary conditions is given. Therefore, it is very difficult to handle the boundary optimization problem by any numerical scheme. In order to stably solve the boundary optimization problem, the TM, one kind of boundary-type meshless methods, is adopted in this study, since it can avoid the generation of mesh grid and numerical integration. In the boundary optimization problem governed by the Helmholtz equation, the numerical solution of TM is expressed as linear combination of the T-complete functions. When this problem is considered by TM, a system of nonlinear algebraic equations will be formed and solved by ECSHA which will converge exponentially. The evolutionary process of ECSHA can acquire the unknown coefficients in TM and the spatial position of the unknown boundary simultaneously. Some numerical examples will be provided to demonstrate the ability and accuracy of the proposed scheme. Besides, the stability of the proposed meshless method will be validated by adding some noise into the boundary conditions.

Keywords: Trefftz method, exponentially convergent scalar homotopy algorithm, boundary optimization problem, Helmholtz equation, boundary-type meshless method, inverse problem.

¹ Department of Harbor and River Engineering & Computation and Simulation Center, National Taiwan Ocean University, Keelung 20224, Taiwan

² Corresponding Author, E-mail: cmfan@ntou.edu.tw

1 Introduction

The boundary optimization problem is one kind of inverse problems. Inverse problems can be found in many realistic engineering applications, such as the detection of vibration phenomena and wave propagation. Many numerical schemes are recently proposed to deal with the inverse problems, such as boundary element methods (BEM) [Marin and Lesnic (2003); Marin (2006)], method of fundamental solutions (MFS) [Mera and Lesnic (2005); Marin and Lesnic (2005)], etc. Since most of the inverse problems are ill-posed, the numerical simulation seems the optimal choice for analyzing the inverse problems. Most of the numerical schemes for inverse problems are very inaccurate, ill-posed and unstable. Therefore, many researchers have paid attention on effectively and stably handling the inverse problems in the past decades [Marin and Lesnic (2003); Marin (2006); Mera and Lesnic (2005); Marin and Lesnic (2005); Barral, Moreno, Quintela and Sanchez (2006); Zou, Zhou, Zhang and Li (2007); Zeb, Ingham and Lesnic (2008); Fan, Chan, Kuo and Yeh (2012); Fan and Chan (2011)]. In this study, a numerical scheme is proposed to stably solve the boundary optimization problem governed by the Helmholtz equation.

In the boundary optimization problem, which is also known as the geometric detection problem, one kind of boundary condition is given on part of boundary, whose positions are unknown *a priori*. And the Cauchy data is given on the rest boundary with known spatial position. There are some numerical schemes have been proposed to handle the boundary optimization problem in recent years. Marin and Lesnic (2003) proposed the BEM and the Tikhonov first-order regularization procedure to deal with the boundary determination problem, while Mera and Lesnic (2005) used the MFS and the Tikhonov regularization to solve three-dimensional inverse geometric problem. Despite of these numerical methods, it is still necessary to develop an efficient numerical scheme for accurately and stably solving the boundary optimization problem. In this paper we propose the Trefftz method (TM) and the exponentially convergent scalar homotopy algorithm (ECSHA) to deal with the boundary optimization problem.

In order to avoid the mesh generation and numerical integration, many meshless methods are proposed recently, such as the MFS [Young, Tsai, Lin and Chen (2006); Gu, Young and Fan (2009)], the radial basis functions collocation method [Duan and Tan (2006); Zhang (2007); Ma and Wu (2009)], the meshless local Petrov-Galerkin (MLPG) method [Atluri and Shen (2002); Atluri, Han and Shen (2003); Atluri, Liu and Han (2006); Li and Atluri (2008); Sladek, Sladek, Sulek and Atluri (2008)], the TM [Abou-Dina (2002); Li (2008); Chen, Lee, Yu and Shieh (2009); Chen, Lee and Shieh (2009)], etc. For the present problem, it is then nature for us to adopt the boundary-type meshless scheme to deal with the

problem, since positions of some boundary points are unknown. The boundary-type meshless methods only need the boundary information rather than the mesh throughout the computational domain. The TM is one kind of boundary-type meshless methods, which are more suitable than the domain-type meshless schemes for the boundary optimization problem. Besides, the numerical solution of TM satisfies the homogeneous governing equation. Its solution is expressed as the linear combination of T-complete functions such that we only require the solution to satisfy the boundary conditions on the collocated boundary points. In this study, the TM is used for spatial discretization of the boundary optimization problem. Since the spatial position of boundary portion is unknown, a system of nonlinear algebraic equations (NAEs) will be formed by satisfying the boundary conditions at every boundary node. The Newton's method is a well-known solver when a system of NAEs is considered. However, the Newton's method is sensitive to initial guessing under certain circumstances. Therefore, some numerical algorithms are proposed in order to stably and efficiently solving the NAEs. Recently, the fictitious time integration method (FTIM) [Liu and Atluri (2008); Chang and Liu (2009); Ku, Yeih, Liu and Chi (2009);] and the scalar homotopy method (SHM) [Liu, Yeih, Kuo and Atluri (2009); Fan, Liu, Yeih and Chan (2010)] have been proposed to efficiently deal with the NAEs. In FTIM, the NAEs are transformed to a system of ordinary differential equations (ODEs) by introducing the fictitious time variable. In SHM, the algorithm also transforms the NAEs to ODEs by introducing the scalar homotopy function and the fictitious time. Based on the above two algorithms, the ECSHA [Fan, Chan, Kuo and Yeih (2012); Fan and Chan (2011); Ku, Yeih and Liu (2010); Liu, Ku, Yeih, Fan and Atluri (2010)] is proposed by using a fictitious time variable and a scalar homotopy function. The convergent rate of the ECSHA is mathematically proven to be exponential. Therefore, we will adopt the ECSHA to efficiently solve the system of NAEs formed by the TM.

In this study, the TM and the ECSHA will be adopted to analyze the boundary optimization problem governed by the Helmholtz equation. The numerical solution of TM is expressed as a linear combination of T-complete functions. Since the coefficients of TM and the spatial position of some boundary points are unknown, a system of NAEs will be formed by forcing the satisfactions of the boundary conditions on boundary collocation points. The unknown coefficients in TM and the position of unknown boundary can be found simultaneously by the evolutionary process of ECSHA. There are some numerical examples provided to demonstrate the ability and accuracy of the proposed scheme. Finally, the stability of the proposed meshless method will be verified by adding some noise into the boundary conditions.

2 Boundary Optimization Problem

The boundary optimization problem considered in this article is governed by the Helmholtz equation. The governing equation and the corresponding boundary conditions are shown as follows:

$$(\nabla^2 + k^2)u(x,y) = 0, \quad (x,y) \in \Omega, \quad (1)$$

$$u(x,y) = q_1(x,y), \quad (x,y) \in \Gamma, \quad (2)$$

$$(\nabla u(x,y)) \cdot \vec{n} = q_2(x,y), \quad (x,y) \in \Gamma, \quad (3)$$

$$u(x,y) = h_1(x,y), \quad (x,y) \in \gamma, \quad (4)$$

$$(\nabla u(x,y)) \cdot \vec{n} = h_2(x,y), \quad (x,y) \in \gamma, \quad (5)$$

where ∇^2 is the Laplacian. k is the wave number, \vec{n} is the unit outward normal vector, and $q_1(x,y)$, $q_2(x,y)$, $h_1(x,y)$ and $h_2(x,y)$ are given boundary conditions. Ω is the interested domain, Γ is the known boundary and γ is the unknown boundary. On the known boundary Γ , overprescribed Cauchy boundary conditions as described in Eqs. (2-3) are given. On the unknown boundary γ , only the Dirichlet or Neumann boundary condition is given, Eq. (4) or (5). The spatial position of γ is unknown *a priori*. The purpose of the boundary optimization problem is to determine the spatial positions of the boundary points on the unknown boundary, γ , and the numerical solution of the Helmholtz problem, $u(x,y)$. The schematic diagram for the boundary optimization problem is demonstrated in Fig. 1(a). For the boundary with unknown spatial position, γ , we will find out the radius of boundary nodes for each fixed azimuth in the polar coordinate system.

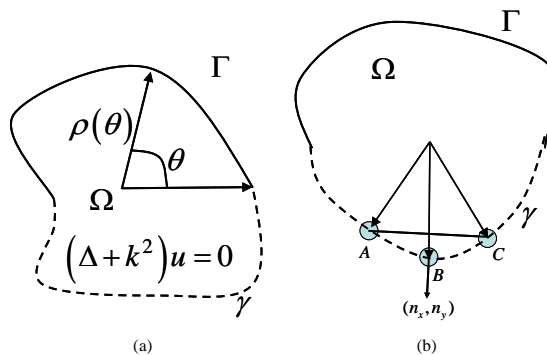


Figure 1: The schematic diagrams for (a) the two-dimensional boundary optimization problem and (b) the unit normal vector.

3 Numerical Method

Since the spatial position of some boundary portion is unknown in advance, it is nature to use the boundary-type meshless method. The TM is adopted for the spatial discretization. In TM, the solution can be expressed by a linear combination of the T-complete functions of the Helmholtz equation with underdetermined coefficients. The unknown coefficients in the expression will then be obtained by enforcing the satisfactions of the boundary conditions for every boundary collocation points.

3.1 The Trefftz method (TM)

The TM for Helmholtz equation will be described in this sub-section. The T-complete functions for Helmholtz equation for the interior domain and doubly-connected domain can be shown in Eq. (6) and Eq. (7), respectively:

$$\{J_0(kr), J_j(kr) \cos(j\theta), J_j(kr) \sin(j\theta), j = 1, 2, 3, \dots\}, \tag{6}$$

$$\{J_0(kr), J_j(kr) \cos(j\theta), J_j(kr) \sin(j\theta), Y_0(kr), Y_j(kr) \cos(j\theta), Y_j(kr) \sin(j\theta), j = 1, 2, 3, \dots\}, \tag{7}$$

where $J_j()$ and $Y_j()$ are Bessel functions of the first kind and the second kind.

For simply- and doubly- connected domains, the numerical solution can be expressed by the T-complete functions listed in Eq. (6) and Eq. (7). The corresponding outer boundary of the computational domain, Ω , in the polar coordinates is given by $\Gamma_0 = \{(r, \theta) | r = \rho(\theta), 0 \leq \theta \leq 2\pi\}$ and the corresponding inner boundary is given $\Gamma_1 = \{(r, \theta) | r = \eta(\theta), 0 \leq \theta \leq 2\pi\}$. The numerical solution of the Helmholtz equation for simply- and doubly- connected domains in TM can then be expressed as the linear combination of the T-complete functions as shown in Eq. (8) and Eq. (9):

$$u(r, \theta) = a_0 J_0(kr) + \sum_{j=1}^m a_j J_j(kr) \cos(j\theta) + b_j J_j(kr) \sin(j\theta), \tag{8}$$

$$u(r, \theta) = a_0 J_0(kr) + c_0 Y_0(kr) + \sum_{j=1}^m a_j J_j(kr) \cos(j\theta) + b_j J_j(kr) \sin(j\theta) + c_j Y_j(kr) \cos(j\theta) + d_j Y_j(kr) \sin(j\theta), \tag{9}$$

where $a_0, c_0, \{a_j\}_{j=1}^m, \{b_j\}_{j=1}^m, \{c_j\}_{j=1}^m$ and $\{d_j\}_{j=1}^m$ are the unknown coefficients which will be retrieved by satisfying the boundary conditions on the boundary collocation points. In Eqs. (8) and (9), terms up to the m -th order are used to replace

the infinite series in the original expressions. Once the unknown coefficients are obtained, the numerical solution and its derivative at any position inside the computational domain can be found from Eqs. (8) and (9). Since the Neumann boundary condition will be given on the unknown boundary, γ , the unit normal vector on γ should be determined via the evolutionary process. In this paper, the out normal vectors at some specific boundary points are approximated from its neighboring nodes as shown in Fig. 1(b). In this figure, the unit outward normal vector at node B is determined from the spatial coordinates of neighboring nodes A and C as

$$(n_x, n_y)_B = \left(\frac{-y_C + y_A}{l_{AC}}, \frac{x_C - x_A}{l_{AC}} \right), \quad (10)$$

where $(n_x, n_y)_B$ is the normal vector at node B. (x_A, y_A) and (x_C, y_C) are the spatial coordinates at node A and node C. $l_{AC} = \sqrt{(x_A - x_C)^2 + (y_A - y_C)^2}$ is the distance between two nodes, A and C. The normal vectors at nodes along γ will vary at every evolutionary step since the spatial positions for boundary points on γ will move at the evolutionary process of ECSHA. It should be noticed that the system of the resulting algebraic equations is nonlinear since the positions for unknown boundary involves in the equations such that the radial distances for boundary points on γ in Eqs. (8) and (9) induce the nonlinearity.

3.2 The exponentially convergent scalar homotopy algorithm (ECSHA)

A system of NAEs will be formed via Eq. (8) or (9) by enforcing the satisfactions of the boundary conditions at boundary collocation nodes. The unknowns in the system of NAEs are both of the coefficients in TM and the spatial positions of boundary γ . For the following NAEs:

$$\mathbf{F}(\mathbf{x}) = \mathbf{0}, \quad (11)$$

where $\mathbf{F} \in R^{ne}$ and $\mathbf{x} \in R^{nn}$. ne and nn are the numbers of equations and unknowns, respectively, it is quite important for us to find a stable and efficient numerical algorithm to solve it. Here we propose to use the ECSHA [Fan, Chan, Kuo and Yeh (2012); Fan and Chan (2011); Ku, Yeh and Liu (2010); Liu, Ku, Yeh, Fan and Atluri (2010)] to solve Eq. (11).

In ECSHA, we consider a scalar homotopy function as follows:

$$h(\mathbf{x}, t) = \frac{1}{2}Q(t)\|\mathbf{F}(\mathbf{x})\|^2 - \frac{1}{2}Q(t)\|\mathbf{F}(\mathbf{x}_0)\|^2 = 0, \quad (12)$$

where t is a fictitious time variable and $Q(t) > 0$ is a given function with $Q(0) = 1$. $\mathbf{x}(0) = \mathbf{x}_0$ is the initial condition. From a series of mathematical derivation [Fan,

Chan, Kuo and Yeih (2010); Fan and Chan (2011); Ku, Yeih and Liu (2010); Liu, Ku, Yeih, Fan and Atluri (2010)], the following evolution equation of ECSHA can be derived

$$\frac{d\mathbf{x}}{dt} = \frac{-\nu}{2(1+t)^d} \frac{\|\mathbf{F}(\mathbf{x})\|^2}{\|\tilde{\mathbf{B}}\mathbf{F}(\mathbf{x})\|^2} \tilde{\mathbf{B}}\mathbf{F}(\mathbf{x}), \quad (13)$$

where ν is the damping coefficient and d is a parameter for convergence rate. \mathbf{B} is the Jacobian matrix with its ij -components given by $B_{ij} = \partial F_i / \partial x_j$. The $\tilde{\mathbf{B}}$ denotes the transpose of Jacobian matrix.

The exponential convergence of ECSHA can be mathematically proved [Fan, Chan, Kuo and Yeih (2012); Fan and Chan (2011); Ku, Yeih and Liu (2010); Liu, Ku, Yeih, Fan and Atluri (2010)] and the ECSHA is insensitive to the initial guess. Hence, we will adopt the ECSHA to efficiently solve the system of NAEs from spatial discretization of TM. For simplicity, the explicit Euler method is used to integrate Eq. (13),

$$\mathbf{x}^{n+1} = \mathbf{x}^n + \Delta t \frac{-\nu}{2(1+t^n)^d} \frac{\|\mathbf{F}(\mathbf{x}^n)\|^2}{\|(\tilde{\mathbf{B}}^n)\mathbf{F}(\mathbf{x}^n)\|^2} (\tilde{\mathbf{B}}^n)\mathbf{F}(\mathbf{x}^n), \quad (14)$$

where the superscripts n and $n + 1$ denote the n^{th} and the $(n+1)^{th}$ time steps. Δt is the time increment for integration. The stopping criterion for Eq. (14) will be defined as:

$$\frac{\|\mathbf{F}^n\|^2}{ne} \leq \varepsilon, \quad (15)$$

where ε is a pre-defined parameter for integration. When $\|\mathbf{F}^n\|^2$ approaches to zero, the solution of Eq. (11) will be obtained.

4 Numerical Results and Comparisons

The boundary optimization problem governed by the Helmholtz equation will be solved by the proposed algorithm which is the combination of TM and ECSHA. In the following subsections, three numerical examples are provided to validate the efficacy and stability of the proposed scheme.

For clarity, the following abbreviations are used in these examples: n_{b1} denotes the number of boundary nodes along Γ , n_{b2} denotes the number of boundary nodes along γ , k denotes the wave number, icb denotes the initial guess of radial distance of the unknown boundary, and icc_1 , icc_2 denote the initial guesses of the unknown coefficients in the solution expression in TM.

2(a). The boundary conditions listed in Eqs. (2)-(3) are prescribed along the upper half boundary, Γ , while the Dirichlet boundary condition is given on the lower part of the boundary, γ . The analytical solution in the first example is expressed as:

$$u(x, y) = \cos(kx) + \sin(ky). \quad (18)$$

Unless otherwise specified, the following parameters are adopted in all of the numerical experiments for this example: $n_{b1} = 30$, $n_{b2} = 20$, $m = 16$, $icb = 1.2$, $icc = 0.1$, $k = \sqrt{2}$, $d = 0.01$, $v = 1$, $\Delta t = 0.01$, $\varepsilon = 10^{-7}$. The numerical (solid line) and analytical solutions (dashed line) are demonstrated in Fig. 3(a), respectively. In addition, the distribution of absolute error is shown in Fig. 3(b). All of the absolute errors are very small which can prove that the proposed scheme can acquire highly accurate solution for the boundary optimization problem.

Since the inverse problem is originated from realistic applications, we add some noise into boundary conditions by the following equations:

$$u(x, y) = q_1(x, y) \left(1 + rd \times \frac{ss}{100} \right), \quad (x, y) \in \Gamma, \quad (19)$$

$$(\nabla u(x, y)) \cdot \vec{n} = q_2(x, y) \left(1 + rd \times \frac{ss}{100} \right), \quad (x, y) \in \Gamma, \quad (20)$$

$$u(x, y) = h_1(x, y) \left(1 + rd \times \frac{ss}{100} \right), \quad (x, y) \in \gamma, \quad (21)$$

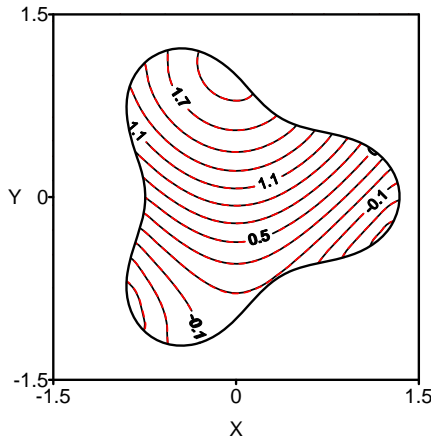
$$(\nabla u(x, y)) \cdot \vec{n} = h_2(x, y) \left(1 + rd \times \frac{ss}{100} \right), \quad (x, y) \in \gamma, \quad (22)$$

where rd is the random number, whose range is $[-1, 1]$. ss is the user-defined parameter to denote the percentage of the noise. The recovered boundary positions by adding different levels of relative noise are shown in Fig. 4. From these results, the spatial positions of unknown boundary can be recovered very well even 1.5% noise level is added into the boundary conditions. It evidently shows the stability and good noise resistance of the proposed scheme. The influence on the numerical accuracy by using different levels of added noise is demonstrated in Table 1(a). From these results, it is proved that the proposed meshless algorithm is very stable and accurate for solving the boundary optimization problem governed by the Helmholtz equation.

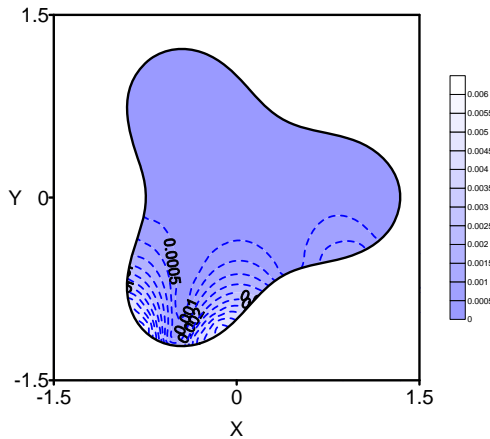
4.2 Example 2

In the second example, the computational domain and boundary are illustrated in Fig. 2(b). The boundary enclosing the computational domain is defined by the parametric equation

$$\Gamma_0 = \{(x, y) | x = \rho \cos \theta, y = \rho \sin \theta, 0 \leq \theta \leq 2\pi\}, \quad (23)$$



(a) numerical solution (solid line) and analytical solution (dashed line)



(b) absolute error

Figure 3: The distributions of (a) numerical solution (solid line) and analytical solution (dashed line), and (b) absolute error.

where

$$\rho(\theta) = 1. \tag{24}$$

All of boundary conditions listed in Eqs. (2)-(3) are prescribed along the upper half boundary, Γ , while the Neumann boundary condition is given on the lower part of the boundary, γ . The analytical solution in the second example is expressed as:

$$u(x,y) = \cos(x) \sin(y). \tag{25}$$

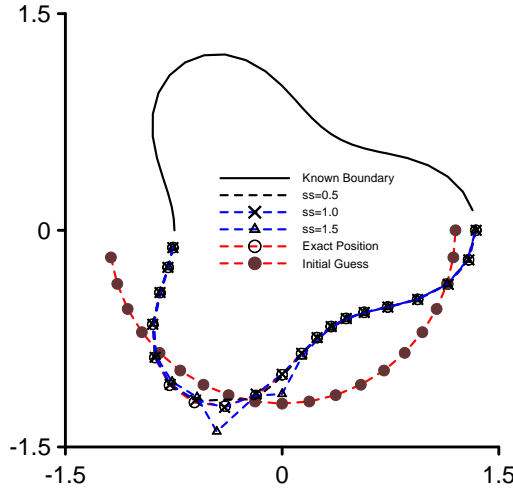


Figure 4: Recovered boundary positions by adding levels of noise.

The following parameters are used in the numerical experiments for this example: $n_{b1} = 34$, $n_{b2} = 16$, $m = 22$, $icb = 0.9$, $icc = 0.2$, $d = 0.01$, $v = 1$, $\Delta t = 0.01$, $\varepsilon = 10^{-7}$. The numerical (solid line) and analytical solutions (dashed line) are demonstrated in Fig. 5(a). Besides, the distribution of absolute error is shown in Fig. 5(b). The recovered positions of unknown boundary portion by adding different levels of noise are depicted in Fig. 6. Although there are little differences between these final positions, the results are acceptable and very stable. In addition, the errors by adding different levels of noise are displayed in Table 1(b). From these numerical results, the proposed meshless scheme is very stable for noisy data and all of the maximum absolute errors are very small.

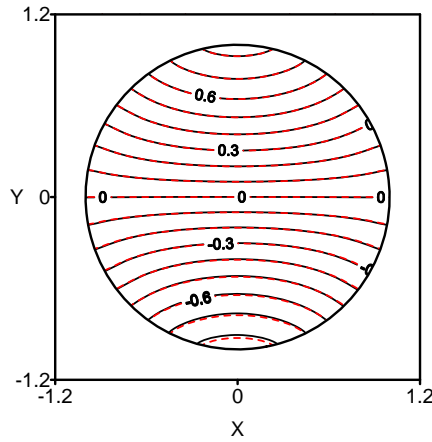
4.3 Example 3

For the third example, the computational domain and boundary are illustrated in Fig. 2(c). The outer boundary enclosing the computational domain is defined by the parametric equation

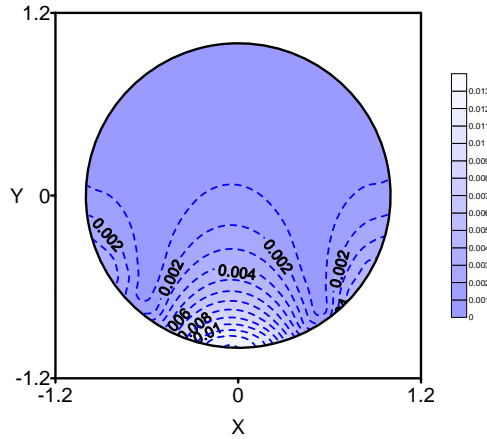
$$\Gamma_0 = \{(x,y) | x = \rho \cos \theta, y = \rho \sin \theta, 0 \leq \theta \leq 2\pi \}, \tag{26}$$

where

$$\rho(\theta) = \left(\cos(3\theta) + \sqrt{2 - \sin^2(3\theta)} \right)^{\frac{1}{3}}. \tag{27}$$



(a) numerical solution (solid line) and analytical solution (dashed line)



(b) absolute error

Figure 5: The distributions of (a) numerical solution (solid line) and analytical solution (dashed line), and (b) absolute error.

The unknown inner boundary, γ , is also a Cassini curve defined as the parametric equation:

$$\Gamma_1 = \{(x,y) | x = \eta \cos \theta, y = \eta \sin \theta, 0 \leq \theta \leq 2\pi \}, \tag{28}$$

where

$$\eta(\theta) = 0.5 \left(\cos(3\theta) + \sqrt{2 - \sin^2(3\theta)} \right)^{\frac{1}{3}}. \tag{29}$$

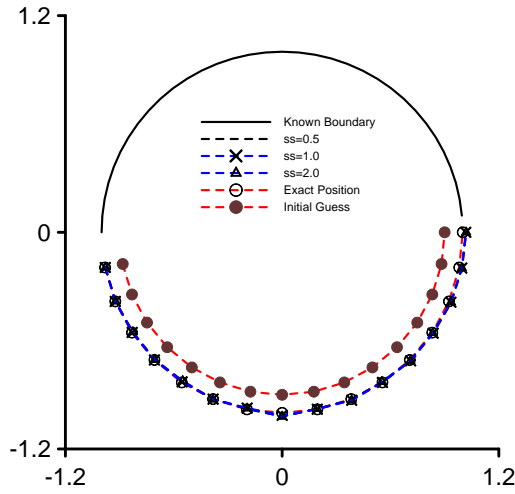


Figure 6: Recovered boundary positions by adding levels of noise.

Table 1: The maximum absolute errors by adding different levels of noise in (a) example 1, (b) example 2, (c) example 3.

(a)

ss	Maximum absolute error
0.5	0.0114
1.0	0.1366
1.5	0.0911

(b)

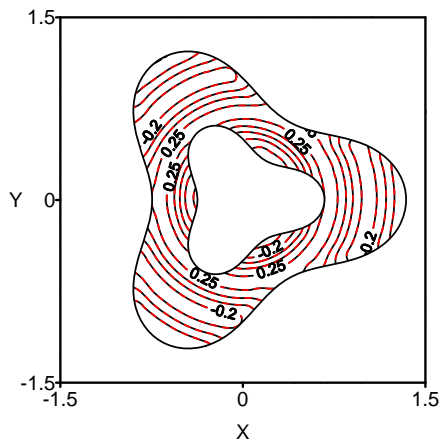
ss	Maximum absolute error
0.5	0.0048
1.0	0.0094
2.0	0.0338

(c)

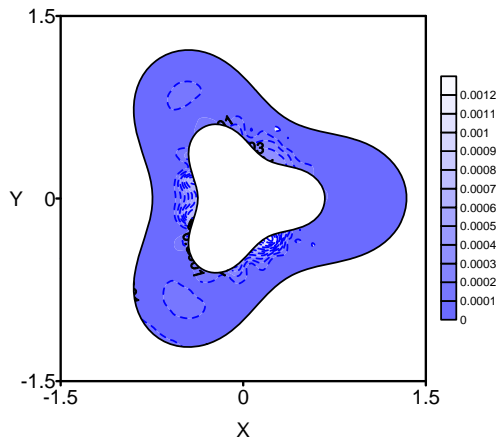
ss	Maximum absolute error
0.5	0.0134
1.0	0.0345
2.0	0.1203

The objective of this problem is to find out the recovered position of inner boundary and the solution inside the doubly-connected domain, while the boundary conditions listed in Eqs.(2)-(3) are prescribed on the outer boundary Γ and Dirichlet boundary condition is given on the inner boundary, γ . The analytical solution in the third example is expressed as:

$$u(x,y) = J_0 \left(10\sqrt{(x-0.02)^2 + (y-0.02)^2} \right). \quad (30)$$



(a) numerical solution (solid line) and analytical solution (dashed line)



(b) absolute error

Figure 7: The distributions of (a) numerical solution (solid line) and analytical solution (dashed line), and (b) absolute error.

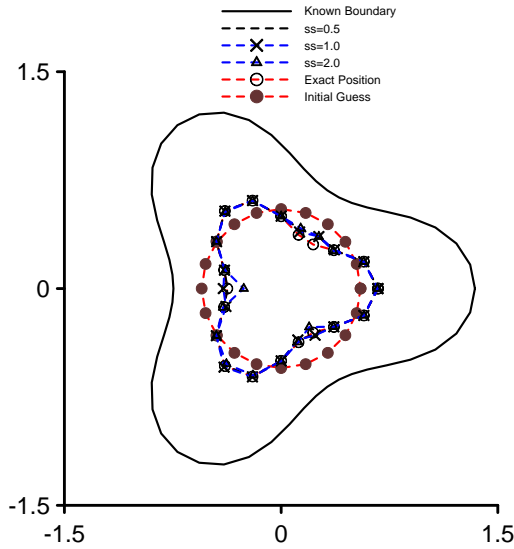


Figure 8: Recovered boundary positions by adding levels of noise.

The following parameters are used in the numerical experiments for this example: $n_{b1} = 50, n_{b2} = 20, m = 9, icb = 0.55, icc_1 = 0.01, icc_2 = -0.01, d = 0.01, \nu = 1, \Delta t = 0.01, \varepsilon = 10^{-7}$. The numerical (solid line) and analytical solutions (dashed line) are demonstrated in Fig. 7(a). In addition, the distribution of absolute error is shown in Fig. 7(b). The recovered positions of unknown boundary portion by adding different levels of noise are depicted in Fig. 8. Besides, the errors by adding different levels of noise are tabulated in Table 1(c). From these numerical solutions, the proposed numerical method is very stable for different levels of noisy data since all of the maximum absolute errors are very small.

5 Conclusions

In this paper, a boundary-type meshless algorithm, the combination of TM and ECSHA, is proposed to stably and accurately analyze the boundary optimization problem which is governed by Helmholtz equation. In the boundary optimization problem, the Cauchy data is given in part of boundary and the Dirichlet boundary condition or Neumann boundary condition is imposed in the other part of boundary whose spatial position is unknown in a prior. The TM is used for spatial discretization for the inverse problem and then it will result in a system of NAEs. The ECSHA is adopted to efficiently solve the system of NAEs. It is insensitive to initial guess and the evolutionary process is proven to be exponentially convergent.

Therefore, the combination of TM and ECSHA is proposed for efficiently solving the boundary optimization problem governed by Helmholtz equation.

There are three numerical examples provided to validate the proposed meshless scheme. By adding different levels of noise into the given boundary conditions, the stability and noise resistance of the proposed method are verified. From all of the numerical results, it can prove that the stability and accuracy of the proposed scheme are excellent. Therefore, it is numerically verified that the proposed meshless method is very stable for solving the boundary optimization problem governed by the Helmholtz equation.

References

Abou-Dina, M.S. (2002): Implementation of Trefftz method for the solution of some elliptic boundary value problems, *Appl. Math. Comput.* vol. 127, pp. 125-147.

Atluri, S.N.; Han, Z.D.; Shen, S. (2003): Meshless local Petrov-Galerkin (MLPG) approaches for solving the weakly-singular traction & displacement boundary integral equations, *Comput. Model. Eng. Sci.*, vol. 4, pp. 507-517.

Atluri, S.N.; Liu, H.T.; Han, Z.D. (2006): Meshless local Petrov-Galerkin (MLPG) mixed finite difference method for solid mechanics, *Comput. Model. Eng. Sci.*, vol. 15, pp. 1-16.

Atluri, S.N.; Shen, S. (2002): The meshless local Petrov-Galerkin (MLPG) method: a simple & less-costly alternative to the finite element and boundary element methods, *Comput. Model. Eng. Sci.*, vol. 3, pp. 11-51.

Barral, P.; Moreno, C.; Quintela, P.; Sanchez, M.T. (2006): A numerical algorithm for a Signorini problem associated with Maxwell–Norton materials by using generalized Newton’s methods, *Comput. Methods Appl. Mech. Engrg.*, vol. 195, pp. 880-904.

Chang, C.W.; Liu, C.-S. (2009): A fictitious time integration method for backward advection-dispersion equation, *Comput. Model. Eng. Sci.*, vol. 51, pp. 261-276.

Chen, J.T.; Lee, Y.T.; Shieh, S.C. (2009): Revisit of two classical elasticity problems by using the Trefftz method, *Eng. Anal. Bound. Elem.*, vol. 33, pp. 890-895.

Chen, J.T.; Lee, Y.T.; Yu, S.R.; Shieh, S.C. (2009): Equivalence between the Trefftz method and the method of fundamental solution for the annular Green’s function using the addition theorem and image concept, *Eng. Anal. Bound. Elem.*, vol. 33, pp. 678-688.

Duan, Y.; Tan, Y.J. (2006): On condition number of meshless collocation method using radial basis functions, *Appl. Math. Comput.*, vol. 172, pp. 141-147.

- Fan, C.M.; Chan, H.F.; Kuo, C.L.; Yeih, W.** (2012): Numerical solutions of boundary detection problems using modified collocation Trefftz method and exponentially convergent scalar homotopy algorithm, *Eng. Anal. Bound. Elem.*, 9. vol. 36, pp. 2-8.
- Fan, C.M.; Liu, C.-S.; Yeih, W.; Chan, H.F.** (2010): The scalar homotopy method for solving non-linear obstacle problem, *Comput. Mater. Con.*, vol. 15, pp. 67-86.
- Fan, C.M.; Chan, H.F.** (2011): The modified collocation Trefftz method for geometry boundary identification problem of heat conduction, *Numer. Heat. Transf. B- Fundam.*, vol. 59, pp. 58-75.
- Gu, M.H.; Young, D.L.; Fan, C.M.**, (2009): The method of fundamental solutions for one-dimensional wave equations, *Comput. Mater. Con.*, vol. 11, pp. 185-208.
- Ku, C.Y.; Yeih, W.; Liu, C.-S.; Chi, C.C.** (2009): Applications of the fictitious time integration method using a new time-like function, *Comput. Model. Eng. Sci.*, vol. 43, pp. 173-190.
- Ku, C.Y.; Yeih, W.; Liu, C.-S.** (2010): Solving non-linear algebraic equations by a scalar Newton-homotopy continuation method, *Int. J. of Nonlin. Sci. Num.*, vol. 11, pp. 435-450.
- Li, S.; Atluri, S.N.** (2008): The MLPG mixed collocation method for material orientation and topology optimization of anisotropic solids and structures, *Comput. Model. Eng. Sci.*, vol. 30, pp. 37-56.
- Li, Z.C.** (2008): The Trefftz method for the Helmholtz equation with degeneracy, *Appl. Numer. Math.*, vol. 58, pp. 131-159.
- Liu, C.-S.; Atluri, S.N.** (2008): A novel time integration method for solving a large system of non-linear algebraic equations, *Comput. Model. Eng. Sci.*, vol. 31, pp. 71-83.
- Liu, C.-S.; Yeih, W.; Kuo, C.L.; Atluri, S.N.** (2009): A scalar homotopy method for solving an over/under-determined system of non-linear algebraic equations, *Comput. Model. Eng. Sci.*, vol. 53, pp. 47-72.
- Liu, C.-S.; Ku, C.Y.; Yeih, W.; Fan, C.M.; Atluri, S.N.** (2010): An exponentially convergent scalar homotopy algorithm for solving a determinate/indeterminate system of non-linear algebraic equations, (submitted).
- Ma, L.; Wu, Z.M.** (2009): Kernel based approximation in Sobolev spaces with radial basis functions, *Appl. Math. Comput.*, vol. 215, pp. 2229-2237.
- Marin, L.** (2006): Numerical boundary identification for Helmholtz-type equations, *Comput. Mech.*, vol. 39, pp. 25-40.
- Marin, L.; Lesnic, D.** (2003): BEM first-order regularisation method in linear elasticity for boundary identification, *Comput. Methods Appl. Mech. Engrg.*, vol.

192, pp. 2059-2071.

Marin, L.; Lesnic, D. (2005): The method of fundamental solutions for inverse boundary value problems associated with the two-dimensional biharmonic equation, *Math. Comput. Model.*, vol. 42, pp. 261-278.

Mera, N.S.; Lesnic, D. (2005): A three-dimensional boundary determination problem in potential corrosion damage, *Comput. Mech.*, vol. 36, pp. 129-138.

Sladek, J.; Sladek, V.; Solek, P.; Atluri, S.N. (2008): Modeling of intelligent material systems by the MLPG, *Comput. Model. Eng. Sci.*, vol. 34, pp. 273-300.

Young, D.L.; Tsai, C.C.; Lin, Y.C.; Chen, C.S. (2006): The method of fundamental solutions for eigenfrequencies of plate vibrations, *Comput. Mater. Con.*, vol. 4, pp. 1-10.

Zeb, A.; Ingham, D.B.; Lesnic, D. (2008): The method of fundamental solutions for a biharmonic inverse boundary determination problem, *Comput. Mech.*, vol. 42, pp. 371-379.

Zhang, Y.X. (2007): Solving partial differential equations by meshless methods using radial basis functions, *Appl. Math. Comput.*, vol. 185, pp. 614-627.

Zou, W.; Zhou, J.X.; Zhang, Z.Q.; Li, Q. (2007): A truly meshless method based on partition of unity quadrature for shape optimization of continua, *Comput. Mech.*, vol. 39, pp. 357-365.